

T- and L-Types of Long-Range Guided Waves for Defect Detection

A. Tatarinov, Evgeny N. Barkanov, E. Davydov and M. Mihovski

Abstract Despite technical advancement and wide industrial application, long-range ultrasonic testing (LRUT) has several bottlenecks, which restrict its abilities and complicate the data interpretation. Particularly, these are related to simultaneous presence along with the main used torsional wave (T-wave) of other wave modes, including longitudinal (L-wave) and flexural (F-wave) ones. The latter are considered as unwanted components, but on the other hand could be a source of additional useful information. The purpose of this study was to use small-scaled models of pipes with simulated defects of different kind to demonstrate some possibilities of signals contrasting for a selected wave mode and sensitivity of T- and L-waves in assessment of these defects. Ultrasonic testing was performed by a specially designed laboratory setup, comprising a data acquisition unit with a waveform generator and an amplifier/digitizer circuitry allowing switching in turn between several transducers pairs. An array of magnetostrictive transducers located stepwise along tubes was arranged, where switching between T- and L-wave excitation modalities was done by changing orientation of the static magnetic field. Experiments were done on thin-walled tubes with diameters of 10 and 45 mm, applying ultrasonic tone-burst pulses with carrying frequency of 125 kHz. Contrast of echo responses from defects for switched in turn T- or L-waves was enhanced by signals processing based on time-shifting of signals from several distantly located transducers along the tube to known time delays for the certain type of wave and further multiplication of the signals amplitudes. The demonstrated efficiency of the approach was in discerning of small defects on the background of parasite components and improved contrasting of large defects. Modeling of several types of defects such as pitting, crevice, and stress corrosion was done by means of mechanical tools. The study showed that different responsiveness of T- and

A. Tatarinov (✉) · E.N. Barkanov
Riga Technical University, Riga, Latvia
e-mail: alta2003@apollo.lv

E. Davydov
E.O. Paton Electric Welding Institute, Kiev, Ukraine

M. Mihovski
Institute of Mechanics of Bulgarian Academy of Science, Sofia, Bulgaria

L-waves to these defects could be a basis for combined use of both modes to characterize the type of defect, depth of penetration through the tube's wall, and expansion along the length. Comparison of T-wave and L-wave responses in the same tube filled by air and water showed that liquid filling not only increased attenuation of the both propagating waves, but also caused significant transformation of echo pattern of L-wave having dispersive nature, while T-wave was more stable. Thus, use of L-wave in LRUT should account for pipes filling by liquid contents.

Keywords Long-range ultrasonic testing (LRUT) · Torsional wave (T-wave) · Longitudinal wave (L-wave) · Corrosion · Modeling · Magnetostrictive transducers

1 Introduction

Application of guided waves in long-range ultrasonic testing (LRUT) of pipelines has a several decade history of research and commercial implementation. From early works in 1970–1990s [1–3], interest to the subject grew and resulted in numerous research papers devoted to theoretical foundation and demonstration of feasibility of the technology [4–7]. The advanced LRUT techniques provided by such manufacturers as Guide Wave Analysis, Guided Ultrasonics Limited, Olympus, Plant Integrity, and others found application in oil and gas industry, as well as in other branches for structural health monitoring of main and technological pipes. Recently issued International Standard ISO 18211:2016 “Nondestructive testing—Long-range inspection of above-ground pipelines and plant piping using guided wave testing with axial propagation” sets definitions and standards for LRUT instrumentation, data collection, and interpretation [8].

In contrast to traditional ultrasonic flaw detection using bulk waves at megahertz frequencies and testing regions in the close vicinity to transducers, LRUT operates with low frequency guided waves, typically in the 30–200 kHz range, traveling long distances along a pipe as a waveguide without sufficient loss of energy. Diagnostic ranges of commercial systems are estimated by tens and even hundreds of meters depending on conditions. Pulse-echo responses from all targets on the way are collected, including reflections from small defects that may be quite weak. The important peculiarity of LRUT is its ability to sense defects that are much smaller (in best resolution cases from 1 to 3% of the pipe's cross-section) than the ultrasonic wavelength, which much exceeds the thickness of pipe's wall and is comparable or even exceeds the pipe's diameter.

Basically, three types of waves propagate in pipes as prolonged hollow thin-walled cylinders: longitudinal (L-wave), torsional (T-wave), and flexural (F-wave), shown schematically in Fig. 1. Although many acoustical modes of different orders are possible, in reality only a few of them are observed in practice.

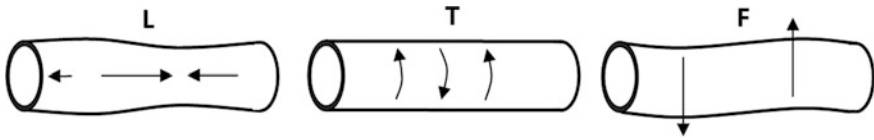


Fig. 1 Schematic illustration of longitudinal (L), torsional (T), and flexural (F) waves in pipes

L-wave or $L(0, 1)$ mode is the fastest wave having similarity to the zero-symmetric Lamb wave S_0 in plates and axisymmetric waves in rods [9]. It is a highly dispersive wave with a strong dependence of the velocity on frequency. T-wave, $T(0, 1)$ mode has the shear origin and its velocity is the same as of the shear wave SH_0 . It has no geometric dispersion, i.e., its velocity is invariant of frequency at any geometrical parameters of a pipe. It is the main advantage of T-wave in LRUT, since its pulses being short and not spreading by distance provide the best axial resolution. Moreover, because of the constancy of T-wave's velocity in pipes made of a certain metal, the distance scale is unambiguously established from the time scale allowing localization of a target along the pipe. F-wave may exist in the form of $F(1, 1)$ mode, which velocity is lower than that of T-wave and depends on the relation of its geometrical parameters to ultrasonic wavelength. Its analogs are flexural or non-axisymmetric waves in rods. This wave is not commonly used in LRUT due to a very dispersive character and a lower sensitivity; however, it is present in echograms as an unwanted component. Dispersion curves for phase and group velocities of different modes of L-, T-, and F-waves are calculated analytically for pipes of a known diameter, wall thickness, and material type. Some examples of such dispersion curves for description of certain pipes are present in the related works [10, 11].

Since its first introduction, the LRUT technology achieved significant progress [12]. Particularly, the achievements included: (i) understanding T- and L-waves, ability of choosing the wave modes and use them at different frequencies to obtain information about the size of a defect; (ii) reducing the size of a detected defect to 3–5% of the pipe's cross-section area; and (iii) introduction of focusing by the length that allowed circumferential location of defects at middle range distances.

At the same time, diagnostic capabilities of LRUT are limited by a number of factors, part of which are hardly overcome due physical reasons and another part represent technical challenges. These factors comprise: (i) sharp damping of ultrasonic signals in pipes buried in sand [13], insulated by plastics and immured in concrete that dramatically reduces the diagnostic range; (ii) energy absorption in fluid filled pipes leading to the same consequences [14]; (iii) difficulty of results interpretation due to multimode propagation and mode conversion at reflection targets (welds, defects) causing false detections; insufficient axial and lateral resolution; (iv) presence of a dead zone; (v) poor ability for detection after the first large target due to signal damping accompanied by the modes conversion and (vi) poor recognition of small pitting defects that impose a serious risk of pipe failure. The testing hardware still remains heavy and complicated requiring labor and time for installation.

The above-mentioned suggests that there is still a room for further improvement of the technology. The purpose of the presented study was to conduct a series of laboratory experiments on small-scaled models of pipes introducing an array of circumferential transducers along the length of a tube. The aims were to demonstrate enhancement of contrast in detection of small defects using a plurality of signals from the array allowing elimination of unwanted modes and to show differences in responses of T- and L-waves from defects of different types. Effect of water filling was also shown.

2 Experimental Setup

To conduct modeling experiments on a smaller scale, a laboratory ultrasonic measurement setup schematically shown in Fig. 2 was constructed. An ultrasonic data acquisition unit comprised a programmable waveform generator with an output amplification circuitry, an input amplifier-digitizer circuitry, and a microprocessor managing data transfer to a computer for processing. Experiments were performed on duralumin tubes with diameters of 10 and 45 mm and wall thicknesses of 1 and 2 mm, respectively, in which defects of different types were simulated artificially by means of mechanical tools. Total lengths of the tubes were 2.5–3 m, corresponding to several dozen of feet in pipes with the natural scale, if to consider the length-to-diameter ratios. Accordingly, the applied ultrasonic wavelengths, time ranges for signals recording, and sizes of ultrasonic transducers were scaled proportionally.

To have a possibility of the selection between the shear and longitudinal acoustic modes purposefully, the magnetostriction principle of ultrasound generating and

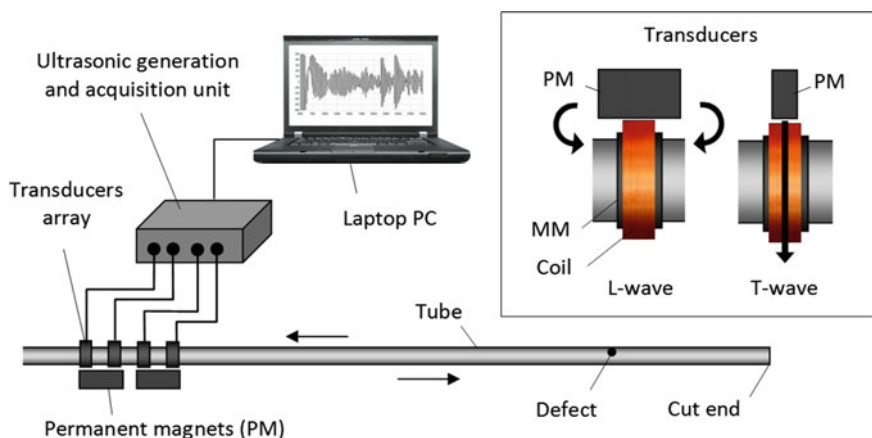


Fig. 2 Experimental setup and layout of transducers arrangement for excitation of L- and T-waves. MM Magnetostrictive metal; *thick arrows* show orientation of static magnetic field

receiving was applied. The method called as EMAT (electromagnetic acoustic transducer) is routinely applied in LRUT as an alternative to the piezoelectric transducers arrays and featured by relative simplicity, lightweight and cost efficiency of the transducer's part [15, 16]. Joule–Villary and Wiedemann effects are utilized to generate respectively longitudinal and torsional waves in tubes. In the first case, the vector of electromagnetic induction of time alternating or oscillating magnetic field is orientated parallel to the same of static magnetic field applied to the magnetostrictive material. In the second case, the vectors of alternating and static magnetic fields are orientated perpendicularly to each other. As the testing tubes in experiments were not ferromagnetic to provide actions of EMAT by itself, 7 mm wide strips of magnetostrictive materials—permendur (iron and cobalt alloy) and nickel were stiffly glued around the tubes by epoxy. The alternating magnetic field was induced in copper wire coils with number of turns 40 wound over the magnetostrictive strips. The static magnetic field was applied by permanent ferrite magnets of rectangular shape sizes $15 \times 10 \times 5 \text{ mm}^3$ put over the coils parallel or perpendicularly to the wire wound, depending on the desirable wave mode, and held by the magnetic force. Four magnetostrictive transducers were arranged along the tube with a step of 25 mm.

Ultrasonic signals were excited by electrical tone-burst pulses applied to the coils. The waveforms were 2-period of sine at a frequency of 125 kHz enveloped by Gauss function and amplified to a voltage of 140 V peak to peak. The acquisition parameters for received signals were as follows: sampling rate of 30 Msps, dynamic range of 10-bit, time frame of 30 ks or about 1 ms in time scale. To acquire signals from different pairs of transducers, the pairs were switched correspondingly. The technical problems to overcome were, first, a low level of signals caused by much weaker ultrasonic outcome of magnetostrictive transducers than of piezoceramic ones and noisiness of acquired signals due to external electromagnetic interferences. The first problem was solved by application of an additional 40 dB preamplifier and electrical matching of the transducers by series connection of capacitors in the excitation and receiving circuits in order to reach resonances in the electrical oscillatory circuits at the applied ultrasonic frequency. To eliminate signals noisiness, the transducers were shielded by grounded foil housings and signals averaging at 256 times.

To observe acoustic modes propagating in the tube at two orientations of the permanent magnet and to determine its velocities, axial profiling by an external piezoelectric transducer with the same work frequency of 125 kHz was undertaken. The coupling was semi-solid plasticine mass permitting reception of both compression and shear oscillations. The resulting hodographs in Fig. 3 show simultaneous presence of all three wave modes—longitudinal (L-wave), torsional (T-wave) and flexural (F-wave) at the both excitation modalities. However, turning of the permanent magnet orientation from L-wave to T-wave helped the relative exaggeration of the torsional mode on the background of other modes. The hodographs demonstrate evidently the lowest dispersion of T-wave signals and no virtual spreading by the distance that beneficially differs from L- and F-waves. The approximate estimates of ultrasound velocities, determined by the hodographs, were

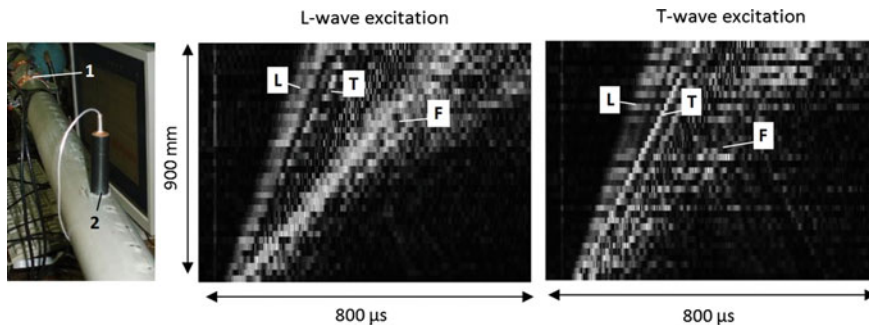


Fig. 3 Ultrasonic profiling of tube: 1 fixed magnetostrictive transducer; 2 piezoelectric receiver traveling stepwise along tube (*left picture*) and time–distance graphs showing hodographs of *L*-, *T*-, and *F*- wave modes at *L*- and *T*-wave excitation modalities

4900 m/s for *L*-wave, 3150 m/s for *T*-wave, and 1950 m/s for *F*-wave. The value for *T*-wave corresponded well to the known tabulated values for the duralumin, while values for *L*-wave (lower than the bulk longitudinal velocity in duralumin 6400 m/s) and *F*-wave were determined by the material and geometrical parameters of the tube and influenced by the geometrical dispersion effects.

3 Enhancement of Contrast in Detection of Small Defects

Enhancement of contrast of helpful pulse-echo signals on the background of parasite signals is important to discern small defects and improve data interpretation. Parasite signals relate to accompanying acoustic modes, for example, *L*- and *F*-waves when tested in *T*-mode. The accompanying modes can occur due to mode conversion upon the reflection of *T*-wave from a certain target or multiple targets in a pipe. The parasite signals propagate at different velocities resulting in a complex interference pattern of the echo response. The most confusing case is the interference between the helpful signal from a small defect with the parasite wave signal from a larger target (weld, edge, support, another defect) having a larger amplitude. The main advantage of *T*-wave is absence of dispersion and ability to propagate over long distances without spreading that provides the best resolution of detection. However, due to the fact that *T*-wave velocity being equal to the same of shear wave is about twice lower than that of the *L*-wave, the first arriving parasite *L*-wave can mask the later arriving *T*-wave. Despite success in designing of special ultrasonic arrays for prevailing generation of *T*-waves, the problem of wave modes conversion at a target remains in effect.

Mathematical processing of several received signals from an array of transducers set at some distance along the pipe is a possible approach to enhance signals propagating only with a known velocity in one direction and scatter all other

signals. Processing of a combination of signals recorded by an array of transducers along a tube included application of corresponding time offsets and further multiplication of the amplitudes. The multiplication procedure was adopted to get equal contributions from all transducer pairs. Algebraic summation would not be appropriate because dissimilarity of bonding and damping of signals passed under glued sensors caused sharp differences of the signal amplitudes in different pairs requiring complicated normalizing. The processing algorithm is presented in Fig. 4. Raw signals from six possible combinations of transducers (including three pairs, two alternating input, and output variants) were recorded and digitized. Time offset or bringing all signals to a common start time applied delays of T-wave propagation between the pairs. The velocity was experimentally predetermined as 3150 m/s corresponding to the shear velocity in duralumin. The differences in distances between pairs were 0, 25, and 50 mm that corresponded to 0, 8, and 16 μ s in time domain. Taking into account that the wave period at 125 kHz was 8 μ s, the signal offsets were comparable and larger than the wavelength. Region of interest was determined in time scale in order to avoid residuals of excitation and unwanted components from farer zones. Amplitudes of 6 time-shifted signals in the region of interest were multiplied. The resulting signal or the product of multiplication was rectified, enveloped by a linear smoothening and displayed. The same procedure was performed also for L-mode applying the corresponding time offsets.

The test object was a 2.5 m duralumin tube with OD = 10 mm, ID = 8 mm, and wall thickness of 1 mm. The array of four transducers was placed approximately in the middle. Two defects simulating pitting corrosion were compared: (i) small defect—a single 0.9 mm diameter through hole in the wall (about 3% of the cross-section area) and (ii) large defects—8 symmetric holes of the same diameter distributed upon the same cross-section (about 24% of the area). The tube's cut end was taken as the reference reflection. The distances from the transducer's array to the defects and the tube's end cut were 92.5 and 105 cm.

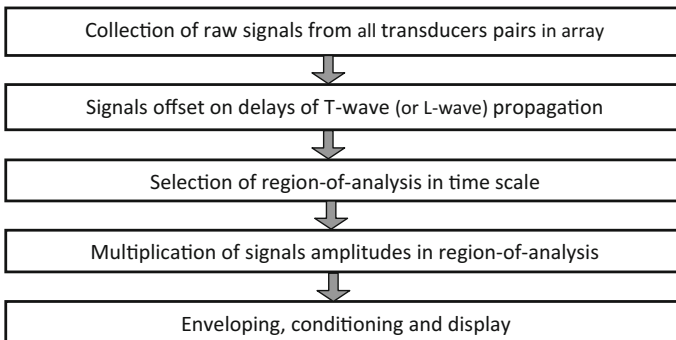


Fig. 4 Diagram of signals processing

Examples of raw signals from an individual transducer pairs and processed echo signals from the plurality of all pairs in the array for T- and L-waves in small and large defects are present in left plots in Figs. 5 and 6. Since the tested length of tube was rather short, echograms obtained by individual pairs of transducers are densely saturated by many interfering signals, where it is difficult to discern separate echo components and understand its origin. Obviously, these are reflections from the both tube's cut ends, defects, and transducers themselves traveling back and forth

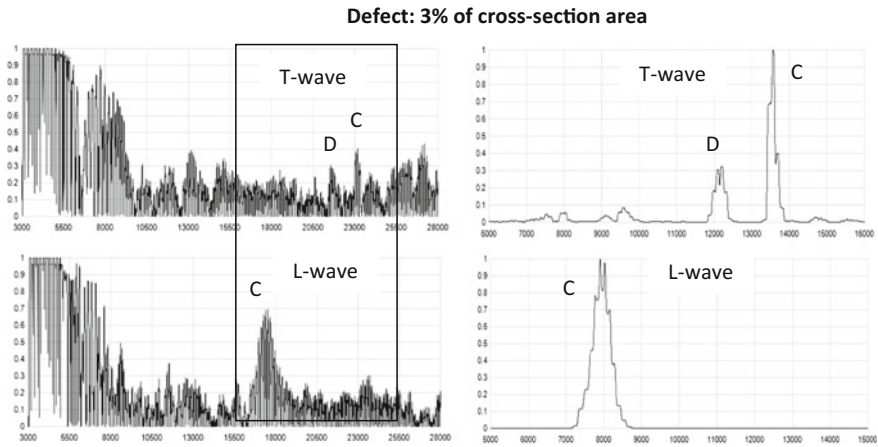


Fig. 5 T- and L-wave responses in the case of small defect (3% of cross-section): *left plots* represent examples of raw signals from a single transducers pairs; *right plots* represent processed signals from all array of transducers in the selected region of analysis marked by rectangle: *D* and *C* are echo peaks from defect and tube's cut end

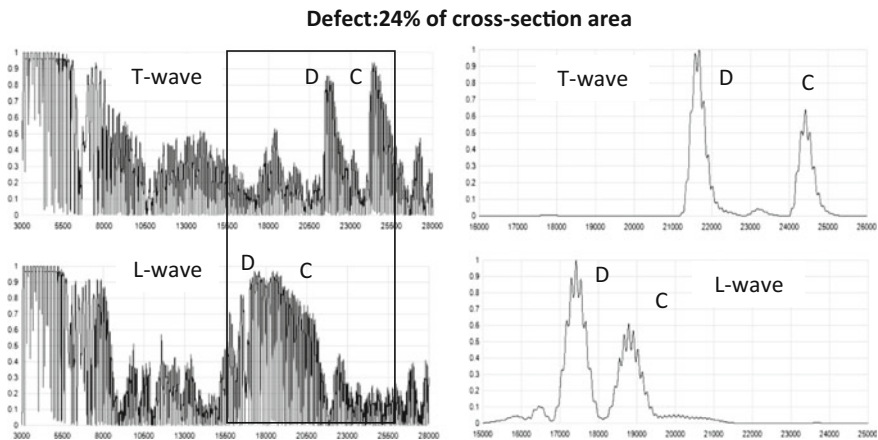


Fig. 6 T- and L-wave responses in the case of large defect (24% of cross-section); indications are the same as in Fig. 5

the tube with different velocities due to relation to different acoustic modes. Locations of responses from defect and tube's end cut can be predicted by real knowledge of the distances and T- and L-waves' velocity. In the case of the large defect, the echo response from it is quite pronounced and the defect can be detected simply by applying a threshold exceeding the average noise level in the region of analysis. However, it is problematic for revealing the small single defect, the response from which is within the average level of acoustic noise and is masked by the latter.

The resulting signals after processing all combinations in the array are present in right plots of Figs. 5 and 6. The amplitudes were normalized by the maximum in the region of analysis. The processing really exaggerated propagation of the helpful signals in selected testing modality and damped all other modes. The reflections from the defect and tube's cut end increased substantially and dominated over parasite modes and reflections coming from the opposite direction along the tube. In the case of small defect, the weak reflection of T-wave from the single defect became prominent on the background, but smaller than reflection of from the tube's end cut. In the case of the large multiple-hole defect, the T-wave reflection from the defect dominated over reflection from the tube's end cut and became absolute over completely suppressed parasite signals. The similar effects were observed for L-wave with the difference that echo pulses of L-wave were more diffuse. In the case of small defect, no L-wave reflection from the defect was observed, while the same of T-wave was quite notable. A defect area of 3% of the cross-section is usually considered as a cut point of resolution for LRUT systems in its real application. The applied processing approach showed an opportunity to lower the resolution threshold in certain cases. Comparison of T- and L-wave responses from a defect may help understanding its size.

Visual comparison of raw and processed signals is shown in Fig. 7 as B-scans, where a line corresponds to a signal in the time scale and brightness codes the amplitude. All signals are present at the same settings of signals conditioning and

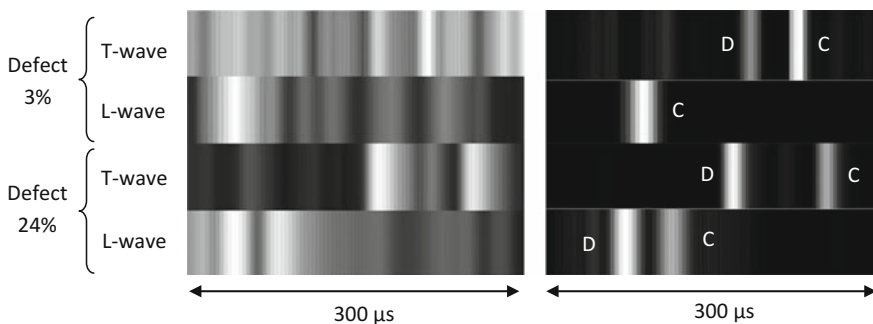


Fig. 7 B-scan presentation of T- and L-wave responses comparing raw (*left*) and processed (*right*) signals in the same region of analysis and at the same contrast of imaging; *D* and *C* are echoes from defect and cut end

imaging contrasting. In raw signals, only the large multiple-hole defect can be surely detected, while the response from small single-hole defect is masked by parasite signals. In the processed signals, only helpful information remained that are responses from small and large defects and the tube's end cut. In the current study, the problem of setting thresholds was solved by normalizing the signals in the presence of a constant target that was the tube's cut end serving as the reference for relative comparison of the amplitudes of responses from the defects. In practice, it can be solved by other reference targets, for instance welds.

Summing, the complex processing proved it helpfulness for the contrast enhancement in LRUT, especially valuable in the case of small defects. Increase of number of transducers in the array can increase the resolution of detection, at one hand, since the more multiplication factors act, the higher is the product, increasing the resolution between the desired modes and parasite signals. On the other hand, this increase is limited by the attenuating action of stiffly glued transducers themselves that damp the propagated guided waves within the array's area. An optimal solution can be obtained experimentally for certain cases.

4 Comparison of T- and L-Modes in Detection of Through and Surface Defects

The aim of this part was modeling different kinds of defects such as pitting corrosion, surface corrosion, and axial cracking observing T- and L-waves responses in each case. Relatively successful attempts to estimate pitting corrosion by guided waves was performed in circumferential testing of pipes at short distances [17]. Although there are some approaches to characterize size and length of defects using L- and T-modes at different wavelengths [5], there is no or almost no practice to identify the type of defect, to describe its expansion by the pipe's depth quantitatively based on the combination of waves. However, a possibility of using a combination of T- and L-waves can be grounded by different intensity of responses of these waves from defects of different geometry.

As mentioned above, a transformed pulse-echo from a defect due to the modes conversion contains longitudinal, torsional, and flexural waves propagating with different velocities and scattering over distance differently. The amplitude ratios between the mentioned modes may vary and be dependent on diverse factors. The difficulty of assessment is caused by spreading of the reflected pulse over the pipe's cross-section by propagation from a local defect along the pipe over a long distance. Another difficulty is the presence of hardly accounted factors of the measurement technology that may overbear effects related to the defect type, for example, uniformity of gluing of magnetostrictive strips to the tube and uniformity of application of the static magnetic field to magnetostrictive transducers.

Although the above-described approach of enhancement signals contrasting was practical for localization of small defects, it came out problematic to use this

processing for comparison of energetic parameters of signals due to distortion and damping of signals passing under transducers in the array. That is why a modified algorithm was applied where locations of defects in the time scale were determined using the contrasting procedure, but energetic characteristics of echo responses from the defects were determined from signals obtained by the nearest transducers pair. The energetic parameter I_d —intensity of the echo from the defect was calculated as the amplitudes integral of the rectified signal in a constant length time “window” around the echo peak. The echo from the tube’s cut end was chosen as the reference reflection, since the size of that target was constant during the experiment, and the corresponding parameter I_c for the echo from the cut end determined. The necessity of the reference reflection was caused by inability to provide a precise reproducibility of the static magnetic field during turning the magnets orientation and, consequently, to provide ideally the same level of excitation of the transducers. A relative value—the ratio of signal integrals of defect and cut end I_d/I_c size was determined to characterize the relative amount of reflected and transmitted energy of ultrasonic pulse interacting with the defect.

Pitting corrosion. Pitting corrosion was modeled by drilling thin through holes in the tube’s wall. In practice, it is the most dangerous type of corrosion manifesting as thin through holes developing across the wall and resulting in leaking. Four stages of the corrosion developments were modeled by gradual doubling the number of through holes symmetrically arranged upon the same cross-section of the tube: 1, 2, 4, and 8. The corresponding metal loss or total defect area S was about 3, 6, 12, and 24% of the tube’s cross-section area or 1.2, 2.5, 5, and 10% of the volume if to account the cylindrical shape of defects. Amplitude integrals for T-wave and L-wave echoes were determined for the zones of defects I_d and the tube’s cut end I_c . The plots of the ratios I_d/I_c dependencies on the total area of defects or metal loss S for T- and L-waves based on the data of four modeled stages are depicted in Fig. 8.

The experimental data showed different character of I_d/I_c dependencies on S for T- and L-waves. The dependence for L-wave has a more linear character, but the

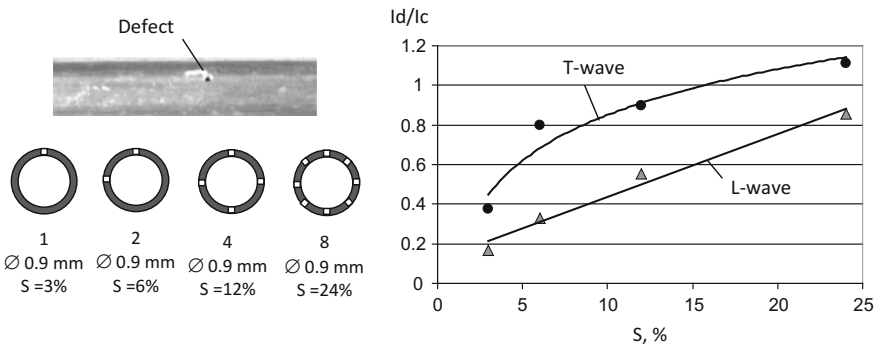


Fig. 8 Model of pitting corrosion and plot of dependence of parameter I_d/I_c on total area of defects S for T- and L-waves

same for T-wave is a strongly nonlinear one with a sharp increment at small values of S . A possible explanation could be that the echo response of L-wave is closer to a laminar character, where the intensity of echo is linearly proportional to the area of reflection, while the T-wave response having the torsional origin is more sensitive to breaking of the cross-section continuity and disruption of its closed circle conducting the torsional mode. Nonlinearity and uneven character of the parameter I_d/I_c in Fig. 8 is explained not only by measurement errors but also by dispersion and spreading of ultrasonic pulses on multiple defects resulting in broad tailing that is seen, for examples, in signals presented in Fig. 6.

Crevice corrosion. In this case, the defects involved only a surface part of the tube's wall penetrating it maximally to a half of the thickness, thus not breaking the entire cross-section. It was considered as a simulation of crevice corrosion that may have similar mechanisms to pitting corrosion but having a less severe form with a more shallow penetration of the tube's wall. Two types of defects were inserted by fine milling: (i) a small notch with a diameter of 2.5 mm and a depth of 0.5 mm and (ii) a prolonged groove along the tube. The groove was 60 mm long, 2.5 mm wide, and 0.3 mm deep. The intensity of T- and L-waves reflections from the defects were normalized by the same from the tube cut end by calculating the parameter I_d/I_c . The result presented in Fig. 9 showed the following findings. Both T-wave and L-wave recognized the single notch (i), but the T-wave's response was much more pronounced than of L-wave. A shallower groove modeling surface corrosion produces a detectable response only by L-wave while the T-wave response remains at the noise level. These data correspond to results described above on modeling pitting corrosion that showed increased sensitivity of T-wave to small defects deeper penetrating the wall. L-wave is more capable to reveal prolonged shallow defects. A combined data on T- and L-waves reflections may help to reveal the type of defect and characterize its expansion upon the wall depth.

Stress corrosion. Stress corrosion cracking occurring in a corrosive environment under tensile stress results in growth of circumferential and longitudinal cracks in pipes. Developing of longitudinal cracks was modeled by axial thin cutting through the entire wall thickness produced by a circular abrasive disk. The length of cutting varied from 10 mm that is comparable to less than a half of ultrasonic wavelength to

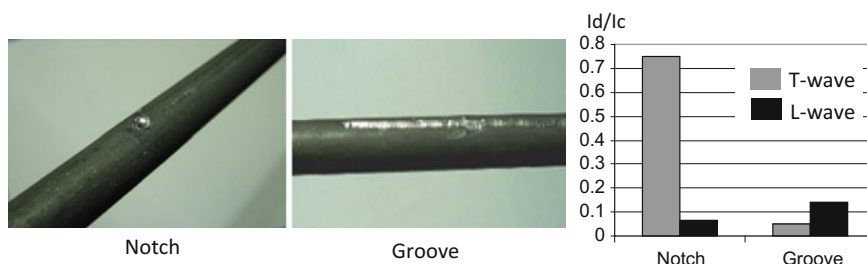


Fig. 9 Models of crevice corrosion and graphical comparison of parameter I_d/I_c in notch and groove types of defects for T- and L-waves

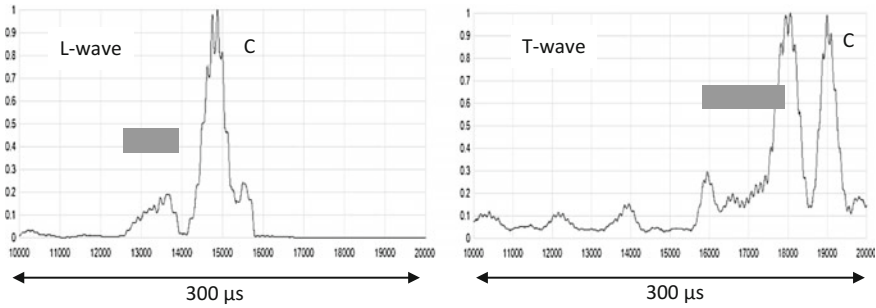


Fig. 10 T- and L-wave echo signals from 110 mm axial thin cutting of tube's wall mimicking longitudinal crack; signals are normalized by amplitude of cut end echo (C); echo responses from axial cutting are marked by rectangles

110 mm or about 4 wavelengths. Both L- and T-wave modes were sensitive to such kind of defects, where short cuts generated single short echoes, but prolonged cuts comparable by the length to 1.5–2 ultrasonic wavelengths and larger generated two pronounced echoes—from the beginning and end points of the cuts. Figure 10 illustrates the example with the longest 110 mm cutting where responses of both T- and L-waves are present. As the reference reflection, the tube's cut end was taken. The similar regularities manifested as for other above-mentioned defects, particularly, T-wave reflection signals are relatively greater than the same of L-wave. It can be explained by the fact that the cutting disturbed the continuity of the section's circle that affected the torsional wave stronger but captured only a small area of the tube's cross-section that had a relatively little effect on the longitudinal or compression wave. Reflection pulses of T-wave from the ends of cutting were lesser dispersed and shorter than of L-wave, producing sharper discerning of the cutting boundaries.

5 Influence of Liquid Filling

The influence of liquid filling was demonstrated by comparing ultrasonic echo signals for switched in turn for T-wave and L-wave modes in an empty or air-filled tube and in the same tube filled with water. The tube's cut ends were similarly sealed in the empty and water-filled conditions to make the results comparable. The targets along the tube were the tube's cut end and a drilled hole simulating a defect located closer to the glued magnetostrictive transducers.

The recorded signals shown in Fig. 11 exhibited obvious differences in the obtained echo patterns for both modes. First, water filling acted as a damper causing a higher attenuation of the reflected signals propagated in the tube due to leakage of ultrasound into water due to a lower differences of impedances between the tube and the medium than in the case of air. Reduction of the echo intensities was by about 1.5 times for T-wave and by more than 2 times for L-wave. Due to a higher

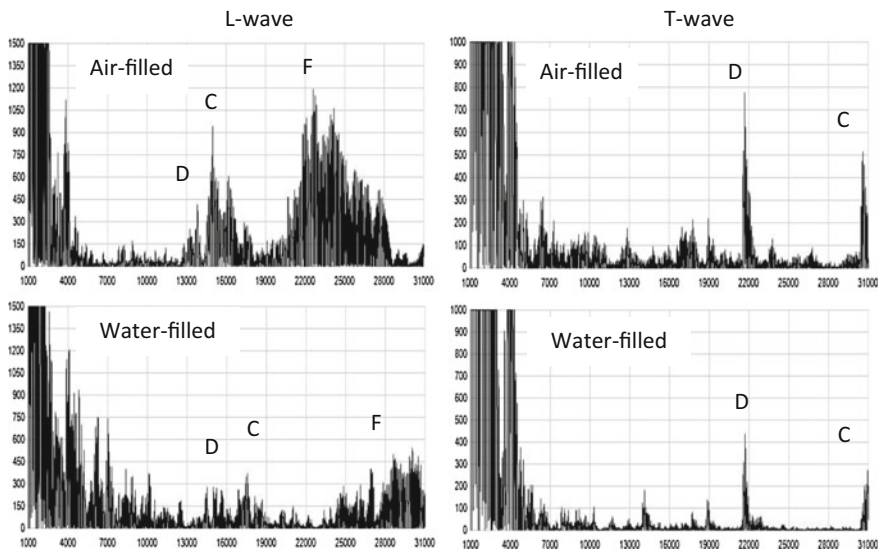


Fig. 11 Illustrations of influence of water filling on T- and L-wave signals in tube: *D* is echo from defect; *C* is echo from cut end; *F* is echo related to F-mode. Signals were obtained at the same settings

degree of damping of longitudinal and flexural modes, the echogram of T-wave in the water-filled tube cleared up from parasite echoes of L- and F-modes and thus the reflections of T-wave from the targets became more contrast in comparison to the empty case, despite lowered amplitudes. The T-wave responses remained practically unchanged in the time scale, while both L-wave and F-wave echoes were delayed. Reduction of velocities of the later modes can be explained by increase of the bulk mass or density of the oscillating system due to water content occurring without increase of its stiffness.

The findings confirmed the necessity to take into account water filling when setting the ranging scale based on the propagation time for different acoustic modes. Variations of the physical properties such as viscosity and density of different liquids and of the same liquid, for instance, under the effect of temperature are capable to affect the velocities. In this view, the most consistent T-wave has an obvious superiority to be used in pipes with liquid fillings.

6 Conclusion

Application of time-shifting and multiplication of echo responses from several transducers arranged stepwise along the length of a pipe can significantly enhance the contrast of desired acoustic modes and damp parasite signals related to other modes that result from the signal conversion or reflections from the opposite

direction. This is an effective measure to increase efficacy of LRUT. Advancement of data processing may include sweeping of the time-shifting in order to account variations of the velocities for different acoustic modes and introduction of calibration for individual pairs of transducers to compensate dissimilarities and attenuation.

Combined use of both T- and L-waves can provide additional information about the type and size of a detected defect, particularly of its development by the depth of the tube's wall and expansion along the length. The study has demonstrated a potential of such approaches based on specific ratios of T- and L-wave responses, however, additional studies are required to investigate quantitative relationships for different types of defects.

Filling the pipe with liquid contents not only creates an increased attenuation of propagating waves, but causes significant transformation of echo patterns, especially of L-waves having dispersive nature, while T-wave keeps stability. In LRUT of pipes filled by liquid contents, the certain type of liquid and its condition should be accounted.

References

1. W. Mohr, P. Holler, IEEE Trans. Ultrason. Ferroelectr. Freq. Control **23**(5), 369 (1976)
2. J.J. Ditri, J. Acoust. Soc. Am. **96**, 3769 (1994)
3. D.N. Alleyne, P. Cawley, IEEE Trans. Ultrason. Ferroelectr. Freq. Control **39**(3), 381 (1992)
4. P. Mudge, Insight **43**, 74 (2001)
5. A. Demma, P. Cawley, M.J.S. Lowe, A.G. Roosenbrand, B. Pavlakovic, NDT Int **37**, 167 (2004)
6. J.L. Rose, Key Eng. Mater. **270**, 14 (2004)
7. M. Sheard, A. McNulty, Insight **43**, 79 (2001)
8. BS ISO 18211:2016. *Non-destructive testing. Long-range inspection of above-ground pipelines and plant piping using guided wave testing with axial propagation* (2016)
9. I.A. Viktorov, *Rayleigh and Lamb Waves* (Plenum Press, New York, 1967)
10. J. Zemanek, J. Acoust. Soc. Am. **51**, 265 (1972)
11. D.N. Alleyne, T. Vogt, P. Cawley, Insight **51**(7), 373 (2009)
12. J.R. Rose, Mater. Eval. **68**(5), 495 (2010)
13. E. Leinov, J.S. Michael, M.J.S. Lowe, P. Cawley, J. Sound Vib. **347**, 96 (2015)
14. H. Sato, H. Ogiso, Jpn. J. Appl. Phys. **53**, 07KC13 (2014)
15. S. Vinogradov, Mater. Eval. **67**, 333 (2009)
16. P. Sun, X. Wu, J. Xu, L. Li, Sensors **14**, 1544 (2014)
17. K. Shivaraj, K. Balasubramaniam, C.V. Krishnamurthy, R. Wadhwan, J. Pressure Vessel Technol. **130**(2), 021502 (2008)

Non-destructive Testing and Repair of Pipelines

Barkanov, E.N.; Dumitrescu, A.; Parinov, I.A. (Eds.)

2018, XVII, 451 p. 280 illus., 100 illus. in color.,

Hardcover

ISBN: 978-3-319-56578-1